Biochar X https://doi.org/10.48130/bchax-0026-0023

Original Research Open Access

Unraveling the microbial ecological mechanisms of different modified biochars for sulfamethoxazole removal in various soils

Caicai Xie[1], Yuye Zhang[1], Tianci Tang[1], Siqi Tong[1], Ruonan Wang[1], Shichao Ma[1], Xiaohui Liu[1*], Fengmin Li[1], Changbing Ye[2], Bin Zhao[2] and Ying Liu[3*]

Received: 2 September 2026

Revised: 7 October 2026

Accepted: 14 October 2026

Published online: 28 October 2026

Abstract

Biochar is widely used to remediate antibiotic-contaminated soils, yet its adaptability across soil types and its impacts on microbial communities remain unclear. Here, we compared three modified biochars (H_3PO_4-modified C1, sixteen alkyl three methyl bromide (CTAB)-modified C2, and $FeCl_3$-modified C3) in black soil and further applied C1 to fluvo-aquic soil and latosol to evaluate the effects of soil type on the removal of sulfamethoxazole (SMX) and bacterial responses via incubation, high-throughput sequencing, network analysis, and PICRUSt prediction. The three soils differed markedly in baseline properties: latosol had the lowest pH and organic carbon, whereas black soil showed the highest enzyme activities under SMX stress. Biochar altered pH, total organic carbon (TOC), enzyme activities, and dissolved organic matter (DOM) composition in a soil-type-dependent manner. C2, enriched in nitrogen and hydrophobic groups, achieved the highest SMX removal in black soil, with SMX removal increasing by 36.5%–37.7% and residual SMX concentrations decreasing to 0.85–1.40 $ng \cdot g^{-1}$. C1 also performed well in black soil and further enhanced SMX removal in fluvo-aquic soil and latosol by 50.2% and 56.9%, respectively. Microbial responses were also soil-specific; biochar reduced bacterial richness most sharply in latosol (Chao1 declined by 67.0%), simplified co-occurrence networks, and shifted keystone taxa from Firmicutes to Proteobacteria at the network level, a shift that was most pronounced in black soil with C2. Taxa previously associated with SMX degradation (*Streptomyces, Micromonospora*, and *Rhodococcus)* were enriched upon the addition of biochar. Phylogenetic investigation of communities by reconstruction of unobserved states (PICRUSt) analysis indicated a predicted restoration of SMX-suppressed carbohydrate, amino acids, and xenobiotic metabolism, with functional recovery being most evident in the acidic latosol. Overall, enhanced SMX removal arises from synergy between abiotic adsorption and biochar-driven microbial restructuring. Soil type influenced the performance of C1, whereas the effects of different modification methods were evaluated in black soil. These findings support a soil-specific biochar matching framework for precise remediation of antibiotic-contaminated soils.

Keywords: Biochar, Sulfamethoxazole, Soil, Remediation, Microbial mechanism

Highlights

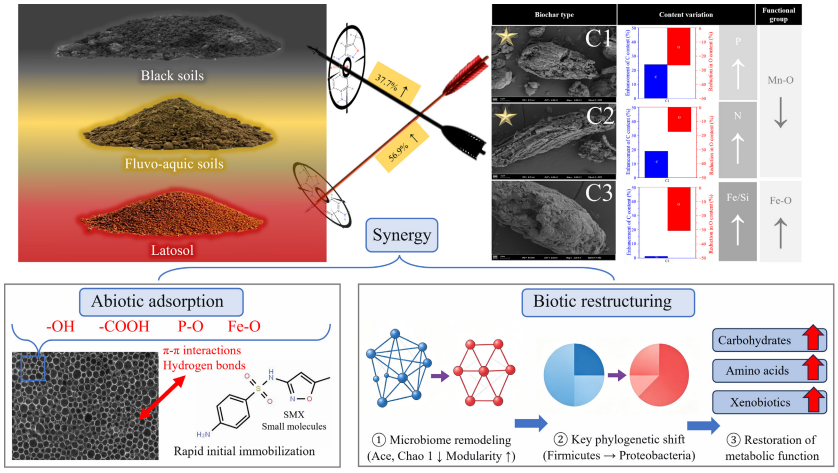
- Soil type strongly influences biochar-driven microbial restructuring and SMX removal.
- Biochar couples abiotic adsorption with microbial network restructuring to enhance SMX removal.
- Biochar simplified microbial networks and enriched SMX-degrading functional taxa.
- SMX increased network complexity, whereas biochar additions reversed this effect.
- A soil-specific framework is proposed for precise biochar selection in remediation.

* Correspondence: Xiaohui Liu (lxh7786@ouc.edu.cn); Ying Liu (liuying8990@qdu.edu.cn)

Full list of author information is available at the end of the article.

https://doi.org/10.48130/bchax-0026-0023

Graphical abstract



Introduction

Sulfonamide antibiotics are widely used for the treatment of pathogenic microbial infections in human and veterinary medicine[1]. However, because of their low metabolic rates[1], these antibiotics are mainly excreted as parent compounds or intermediate metabolites and persist in the environment[2]. Sulfamethoxazole (SMX) is one of the most widely used sulfonamide antibiotics because of its low cost and efficacy[2]. It is often found at high levels in environmental matrices and is highly persistent in soil environments[3–5]. The accumulation of SMX in agricultural soil raises a potential risk to human health via the food chain, prompting international concern[6].

Carbon-based materials such as activated carbon, porous carbon, carbon nanotubes, graphene oxide, and their derivatives have been identified as potential candidates for soil remediation because of their large specific surface area, superior adsorption capacity, and environmental compatibility[7]. Among these materials, biochar is a cost-effective carbonaceous material obtained from the pyrolysis of biomass and is extremely effective in removing organic pollutants in contaminated soils, including antibiotics. For example, Srinivasan et al.[8] showed that a pine wood chip biochar could remove up to 72.9% of SMX. Rajapaksha et al.[9] found that the addition of 5% echinocactus biochar reduced sulfadiazine uptake by lettuce roots by 86%. Appropriate biochar modification methods can lead to greater adsorption of antibiotics in the soil[10].

However, the adsorption efficiency of biochar is mainly dependent on various soil properties such as the pH, organic matter content, soil texture, and mineral composition[11]. These factors modulate interactions between the biochar's surface and antibiotic molecules, as well as the subsequent microbial degradation processes. Importantly, the heterogeneity of soil, as reflected in the pronounced variability among different regions of China, constitutes an important source of variation in the remediation effectiveness of biochar[11,12]. For instance, biochar's performance in acidic red soils in southern China can significantly differ from that in alkaline soils in the north, as well as between organic black soils and sandy fluvo-aquic soils[13]. Recent studies have shown that machine learning algorithms are effective in predicting the remediation effects of biochar on cadmium-contaminated soils, and the soil's physicochemical properties explain about 19.44% of the variation in remediation results, indicating the importance of soil properties in the regional application of biochar[11].

In addition to adsorption capacity, the application of biochar can change the physical, chemical, and biological properties of soils, resulting in improvements in soil fertility, nutrient cycling, and the microbial community's structure[14]. The effects of biochar on soil biota have received much attention because of its importance to the ecological stability and functionality of the soils. However, the effects of biochar on microbial abundance and diversity are not always consistent. For instance, Wang et al.[15] showed that the addition of biochar increased microbial abundance in the rhizosphere, whereas Xu et al.[16] found a decrease. These differences are probably related to the differences in the physicochemical properties of the soil, which can modulate the ecological effects of biochar[17]. Several studies have reported that biochar can increase bacterial diversity and change the community structure at different taxonomic levels, probably by changing the microenvironment of soil, thereby affecting the transport and transformation of nutrients and contaminants[18,19].

Biochar plays a dual role as an adsorbent and a soil conditioner. It not only immobilizes antibiotics but also modulates the microbial community's composition, which may affect the biodegradation efficiency of contaminants such as SMX. Although many studies have explored the adsorption mechanisms of biochar in aquatic and soil environments, the environmental behavior of modified biochar and the corresponding microbial responses after its application in antibiotic-contaminated soils, especially in different soil types, are still insufficiently studied. Here, H_3PO_4, hexadecyl trimethyl ammonium bromide (CTAB), and $FeCl_3$ were selected as modifiers because they represent three typical and mechanistically complementary strategies (acid functionalization[20,21], cationic surfactant-mediated hydrophobization[22,23], and metal oxide loading[24,25]). These strategies target key SMX adsorption mechanisms, including hydrogen bonding and surface complexation, hydrophobic partitioning, electrostatic attraction, metal complexation, and ligand exchange[20,22,24]. They also have well-established preparation methods and are relatively low-cost, allowing their comparison under identical conditions. Their theoretical differences in surface charge, pore structure, hydrophobicity, and SMX adsorption mechanisms are detailed in Supplementary Table S1.

Given these differences, we propose three hypotheses: (1) H_3PO_4-, CTAB-, and $FeCl_3$-modified biochars differ in their SMX adsorption mechanisms and removal efficiency because of their distinct surface charge, pore structure, hydrophobicity, and functional groups. (2)

Soil type regulates biochar's effects on SMX removal, enzyme activities, dissolved organic matter (DOM) composition, and bacterial communities by altering SMX's speciation, biochar's surface charge, and microbial habitats, so no single modified biochar is universally optimal. (3) Modified biochar enhances SMX removal through a synergistic mechanism combining abiotic adsorption and immobilization with microbial community restructuring, including simplified co-occurrence networks, enriched SMX-degrading taxa, and recovery of predicted metabolic functional potential, with these responses jointly controlled by the soil type and modification method. Through incubation, high-throughput sequencing, network analysis, and phylogenetic investigation of communities by reconstruction of unobserved states (PICRUSt) prediction, this study aimed to reveal how modified biochar affects SMX removal, soil properties, and microbial communities in different soils, providing a basis for soil-specific biochar selection in the remediation of antibiotic-contaminated soil.

Materials and methods

Soil sampling sources and physicochemical properties

This study selected surface soil samples (0–20 cm) from farmland in Heilongjiang, Shandong, and Hainan, representing typical agricultural soil types in China: black soil (B), fluvo-aquic soil (Y), and latosol (R). The physicochemical properties of these three soil types differ significantly. Black soil (B) has a neutral pH and a high organic carbon content, representing typical agricultural soils in North China; fluvo-aquic soil (Y) is neutral to alkaline with a moderate organic carbon content, serving as the primary cultivated soil in East China; and latosol (R) is acidic with a relatively low organic carbon content, representing the tropical/subtropical soils of southern China. Given the pH and organic carbon gradients established using these soils, the remediation efficacy of biochar against agricultural antibiotic pollution under different farmland environments can be systematically evaluated. After field collection, soil samples were uniformly air-dried, mixed, lightly ground, and sieved through a 2-mm mesh. Soil pH was determined by the potentiometric method at a soil-to-KCl (1 mol·L^{-1}) ratio of 1:2.5 (w/v) using a pH meter (DELTA320, METTLER TOLEDO, Switzerland). Total organic carbon (TOC) was measured using a TOC analyzer (TOC-L CPH, Shimadzu, Japan). The basic physicochemical properties of the soils are summarized in Supplementary Table S2.

Preparation and characterization of biochar

The *Phragmites australis* used in this study was obtained from the constructed wetland and was selected because of its low cost and adaptability. The collected *P. australis* was washed with deionized water and dried in a blast-drying oven at a constant temperature of 45 °C. The dried *P. australis* was ground to a size that passed a 200-mesh to facilitate granulation and pyrolyzed at 550 °C for 2.5 h in a muffle furnace under a nitrogen atmosphere. The resulting biochar was cooled to room temperature to obtain the original biochar.

The pristine biochar was modified using three different agents to prepare H_3PO_4-, CTAB-, and $FeCl_3$-modified biochars (designated C1, C2, and C3, respectively). They represent several different biochar modification strategies that have been widely reported. Acid functionalization was accomplished using H_3PO_4; the hydrophobic surface modification was carried out using CTAB; and the metal oxide loading used $FeCl_3$. The general procedure involved mixing the biochar with the solution for modification, shaking, separation, washing, drying, and grinding. For the H_3PO_4 modification (C1), 5 g of pristine biochar was mixed with a 20% (v/v) H_3PO_4 solution at a solid-to-liquid ratio of 1:10 (w/v). The mixture was shaken at 200 rpm and 25 °C for 24 h. The solid product was separated by vacuum filtration and rinsed repeatedly with deionized water until the filtrate had a neutral pH. The biochar was oven-dried to a constant weight, ground, and sieved through a 100-mesh sieve before storage in a desiccator. The procedures for preparing C2 (CTAB-modified) and C3 ($FeCl_3$-modified) were identical to that for C1 except that the modifying solution was different. Specifically, C2 was prepared by mixing 5 g of pristine biochar with 200 mL of a 10 g·L^{-1} CTAB solution, whereas C3 was prepared by immersing 5 g of pristine biochar in 50 mL of a 0.5 M $FeCl_3$ solution. Both suspensions were shaken under the same conditions (200 rpm, 25 °C, 24 h). H_3PO_4, CTAB, and $FeCl_3$ were of analytical grade and were purchased from Sinopharm Group Co. Ltd. (China).

The surface morphology and structure of the biochar were examined by scanning electron microscopy (SEM) (Gemini300, Zeiss, Germany). The elemental composition of the biochar was further analyzed by energy-dispersive X-ray spectroscopy (EDS) in point-scan mode under a focused electron beam. The functional groups of biochar were investigated by Fourier transform infrared (FT-IR) spectroscopy (Nicolet iS5N, Thermo Scientific, USA) using the potassium bromide (KBr) pellet method. Briefly, dried biochar was finely ground and mixed with spectroscopic-grade KBr at a mass ratio of 1:150 (biochar–KBr), and the mixture was then pressed into transparent pellets under a vacuum. Fourier transform infrared spectroscopy (FTIR) spectra were recorded over the wavenumber range of 400–4,000 cm^{-1} with a resolution of 2 cm^{-1}, and 32 scans were accumulated for each sample.

Experimental design and soil incubation with SMX

To investigate the remediation effects of different modified biochar on SMX-contaminated soils and the microbial response mechanisms, a microcosm experiment was conducted. Eleven treatments were designed with three replicates each (details in Supplementary Table S3), including blank controls of the three soil types (CKB, CKY, and CKR, corresponding to black soil, fluvo-aquic soil, and latosol, respectively), SMX-contaminated controls (BA, YA, RA), and biochar-amended treatments. Specifically, three modified biochars (C1, C2, C3) were added to black soil (BCA1, BCA2, BCA3) to evaluate the impact of different biochar modification methods on SMX remediation. Although C2 exhibited the highest SMX removal rate in black soil, C1 also performed well (see section *Enhanced SMX removal and soil property changes by modified biochar*), and C1 represents an acid-functionalized treatment with pH-dependent surface chemical properties (Supplementary Table S1), which is particularly important for testing the effects of soil type. Therefore, C1 was selected for cross-soil comparisons and applied to fluvo-aquic soil and latosol (YCA1, RCA1). The performance of C1 across different soil types was evaluated by comparing the BCA1, YCA1, and RCA1 treatment groups. SMX (purity > 98%) was purchased from ANPEL (Shanghai, China).

For each treatment, 60 g of soil (dry weight equivalent) was added to a 100-mL conical flask. Soil moisture was adjusted to 60% of field capacity, and the soils were pre-incubated at 25 °C for 10 d to reactivate microbial activity. Then a SMX standard solution was added to the designated treatments to reach a final concentration of 20 ng·g^{-1}. At the same time, 0.6 g of the corresponding modified biochar (1%, w/w) was added to the biochar-amended treatments and mixed thoroughly. Soils were incubated for 90 d at 25 °C under a 12-h photoperiod, with the water content kept constant by weighing and adding water throughout the incubation period.

Destructive sampling was conducted on Days 30, 60, and 90 to determine the residual concentrations of SMX. Soil samples for microbial community analysis were collected on Day 90.

Measurement of soil properties, enzyme activities, and SMX content

Three-dimensional fluorescence spectra of the soil samples were recorded on a fluorescence spectrophotometer (F-7000, Hitachi, Japan) with a 1-cm quartz cuvette. The excitation wavelength ranged from 200 to 450 nm and the emission wavelength from 250 to 600 nm, with slit widths of 5 nm for both excitation and emission, and a scan speed of 12,000 nm·min^{-1}. The photomultiplier Tube (PMT) voltage was set to 700 V. Raman and Rayleigh scattering were eliminated by subtracting blank water spectra and manual zeroing. Parallel factor analysis (PARAFAC) was performed using the DOMFluor toolbox in MATLAB 2019 to identify the fluorescent components of DOM[26,27]. Details are provided in Supplementary Text S1.

To determine soil enzyme activity, sucrase activity was measured using the 3,5-dinitrosalicylic acid colorimetric method, urease activity was measured using the indophenol blue colorimetric method, and phosphatase activity was measured using the disodium phenylphosphate colorimetric method[28]. All enzyme activities are expressed relative to the weight of dry soil. Details are provided in Supplementary Text S2.

The concentration of SMX was analyzed using a high-performance liquid chromatography–tandem mass spectrometry (HPLC-MS/MS) system (8040, Shimadzu, Japan). The mobile phase composition and flow rate were optimized according to previous research[29]. Details are provided in Supplementary Text S3.

DNA extraction and MiSeq sequencing

For microbial community analysis, soil samples were collected at the end of the incubation period (Day 90). The samples were subsequently homogenized for DNA extraction using the FastDNA® Spin Kit for Soil (MP Biomedicals, France). Then the extracted DNA was stored at −20 °C in 20 μL of a Tris-EDTA (TE) buffer. The bacterial *16S* rRNA V3–V4 region was sequenced utilizing the Illumina MiSeq platform (Shanghai Majorbio Bio-Pharm Technology Co., Ltd., Shanghai). Operational taxonomic units (OTUs) were delineated at a 97% similarity threshold, a standard criterion in microbial community analysis, facilitating robust bioinformatic analysis.

Statistical analysis

To evaluate the effects of modified biochar and soil type on SMX removal and the microbial community's composition, a combination of univariate statistics, diversity indices, and molecular ecological network analysis was applied. Alpha-diversity indices such as Shannon's, Simpson's, abundance-based coverage estimator (ACE), and Chao1 were calculated and tested using standard statistical procedures. One-way analysis of variance (ANOVA) followed by Tukey's honestly significant difference (HSD) test ($p < 0.05$) was applied to evaluate significant differences in SMX concentrations, soil physicochemical properties, and diversity indices among treatments. Beta diversity was evaluated by principal coordinate analysis (PCoA) based on Bray–Curtis distances at the OTU level, combined with permutational multivariate analysis of variance (PERMANOVA) to test the significance of differences among groups. The homogeneity of multivariate dispersions was assessed using the betadisper function with 999 permutations before interpreting the PERMANOVA results. Differential abundance analysis at the phylum and genus levels was performed using analysis of compositions of microbiomes with bias correction 2 (ANCOM-BC2) to account for the compositional nature of *16S* rRNA genes' sequencing data. Holm-adjusted q-values were used to control the false discovery rate, and taxa with $q < 0.05$ were considered to be differentially abundant. Log fold changes are reported on the natural log scale.

The molecular ecological network analysis (MENA) was based on OTU data obtained from high-throughput sequencing. Network construction and analysis were conducted using the random matrix theory (RMT)-based model on the MENA online platform (http://ieg4.rccc.ou.edu/MENA/login.cgi)[30], and the results were visualized using Cytoscape 3.6.1. Modularity-based partitioning was applied to categorize nodes and edges, with distinct colors representing bacterial phyla identified by the OTUs.

Results

Physicochemical characteristics of biochar

The physicochemical properties of biochar are presented in Supplementary Table S4. The pristine biochar was neutral, whereas modifications with phosphoric acid and iron significantly reduced the pH. This acidification is attributed to the hydrolysis of iron compounds, which releases protons, and the consumption of the surface's basic functional groups during modification. In addition, obvious differences in both composition and relative content of surface elements were observed between the pristine and modified biochars (Fig. 1a). Specifically, compared with the pristine biochar (C: 45.23%, O: 42.90%), the carbon mass fraction increased in C1 (69.38%) and C2 (64.05%) but only slightly in C3 (46.48%). In comparison, the oxygen mass fraction of all the modified samples was significantly reduced, especially in C3 (12.25%) and C1 (16.49%). Previous studies have reported that the lower oxygen content is detrimental to the formation of water molecule clusters on the surface functional groups, thereby improving the capacity of the biochar to adsorb organic pollutants[31]. For C1, the phosphorus (P) mass fraction significantly increased from 0.04% to 0.98%, indicating the successful loading of phosphate-containing groups on the surface. Similarly, C2 showed a significant increase in nitrogen (N) content from 0.68% to 3.04%, which is ascribed to the grafting of nitrogen-containing functional groups from CTAB. The content of iron (Fe) increased almost four times for C3, and the content of silicon (Si) reached 38.26%, indicating an efficient loading of Fe and the retention of the original silica matrix.

The FTIR spectra of all biochar samples showed a characteristic band at 3,442 cm^{-1} (O–H stretching), 2,972 cm^{-1} (C–H stretching), 1,614 cm^{-1} (aromatic C=C and C=O stretching), and a minor band at 2,362 cm^{-1} caused by the atmospheric CO_2 (Fig. 1b). These bands showed slight changes in shape and intensity after modification with H_3PO_4 or CTAB, indicating the limited effects of these treatments on the bulk structures of hydroxyl groups, methyl groups, and aromatic domains. The FTIR spectrum of the pristine biochar showed characteristic bands at 1,395 cm^{-1} (C–H deformation), a broad band at 1,088–1,046 cm^{-1} (C–O stretching), and a band at 886 cm^{-1} (M–O stretching, where M = metal or Si).

The infrared spectra of the biochar after modification with CTAB and H_3PO_4 mainly preserved the characteristic features of the pristine material, with only minor changes in peak intensity or position, except that the C–H bending band at 1,395 cm^{-1} disappeared and the M–O band at 886 cm^{-1} was significantly weakened. This suggests possible interactions of the CTAB and the phosphate groups with the C–H and M–O sites, which might have resulted in the removal of surface metal impurities during modification. Conversely, C3 exhibited different spectral changes. A new aliphatic C–H stretching band appeared at 2,902 cm^{-1}, and the C–H bending

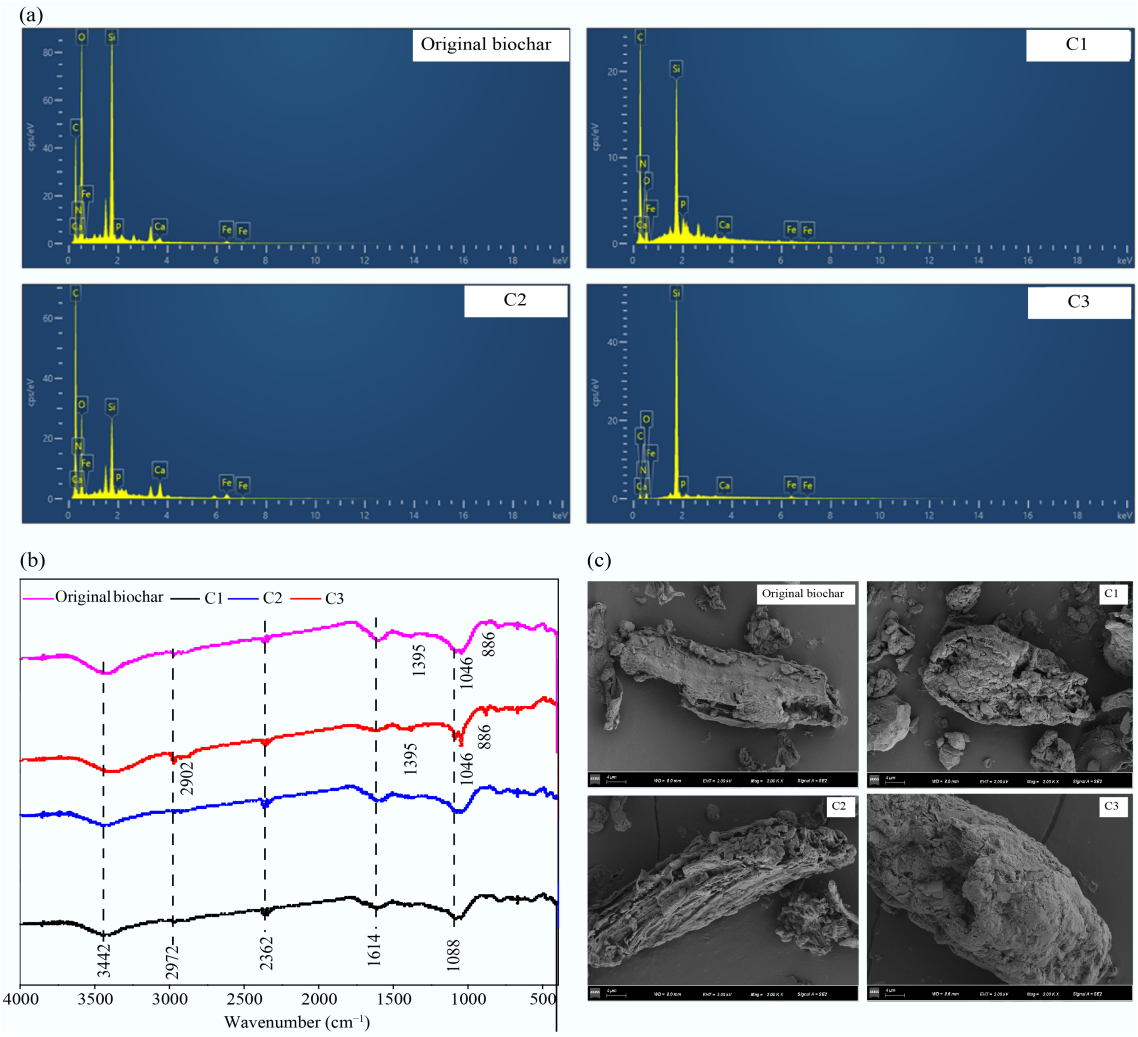


Fig. 1 Characterization of the biochar. (**a**) EDS characterization of original and modified biochars. (**b**) Infrared spectra of original biochar and modified biochars. (**c**) SEM images at low magnification (2.0 k).

(1,395 cm^{-1}) and C–O stretching (1,046 cm^{-1}) bands were augmented. The peak at 1,046 cm^{-1} also became sharper, indicating that the iron modification introduced relevant functional groups, increasing their relative content. Furthermore, a new peak attributable to Fe–O bending vibrations emerged near 886 cm^{-1}. This observation suggests that iron was loaded onto the biochar surface, possibly in the form of Fe–O groups.

Figure 1c and Supplementary Fig. S1 present the SEM images of the pristine biochar and the three modified biochars. The pristine biochar exhibited a relatively smooth and compact surface, characterized by a bundled structure with small attached particles. However, the modified biochars had more obvious surface textures and detectable pore structures, indicating the variation of the modification methods on the surface properties of the biochar. C1 exhibited an ellipsoidal morphology and appeared to have a more developed pore structure, whereas C2 showed more evident surface pores. These observations are consistent with previous studies in which phosphoric acid activation increased porosity through cellulose swelling and the introduction of phosphate groups[20], and CTAB modification increased the average pore size and total pore volume[22]. C3, in contrast, had a rougher surface covered with fine particles. EDS showed a marked increase in the Fe content of C3, suggesting that iron species were deposited on the biochar's surface, possibly as iron (hydr)oxides. Zeng et al.[24] also confirmed via X-ray diffraction (XRD) that activation of $FeCl_3$ leads to the formation of iron oxides such as Fe_2O_3, Fe_3O_4, and Fe^0 on the biochar's surface. Several studies have shown that such structural changes substantially improved surface porosity and helped in pollutant adsorption. C2 deposited granular substances on its surface, resulting from the long carbon chains of the surfactant. Such surface modification increased the hydrophobic active sites, resulting in a 13.5% enhancement in efficiency of removing organic pollutants[23]. Conversely, C1 increased surface porosity but reduced pore volume, which led to a significant 33% improvement in efficiency of SMX adsorption[21]. Furthermore, C3 lowered the biochar's pH and roughened its cross-sectional morphology, which contributed to an 11% increase in the capacity for arsenic adsorption[25].

Enhanced SMX removal and soil property changes caused by modified biochar

To study the effect of modified biochar on the removal of SMX in contaminated soils, we compared the effects of different biochar modification methods on changes in the SMX concentration in black

https://doi.org/10.48130/bchax-0026-0023

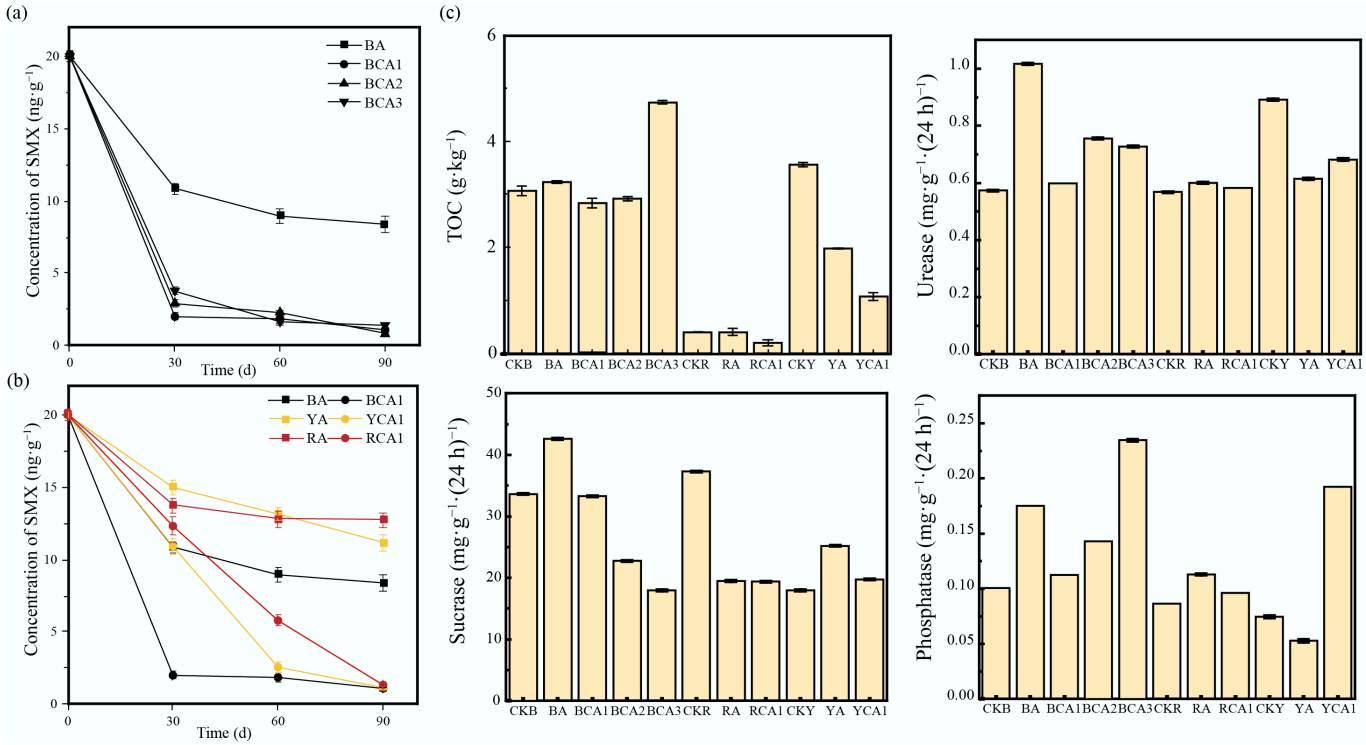


Fig. 2 Enhanced removal of SMX by modified biochar in contaminated soils and the corresponding changes in soil TOC and enzyme activities. (**a**) Comparative effectiveness of different biochars in black soil. (**b**) Performance of C1 in different soil types. (**c**) Soil TOC and enzyme activities under different treatments.

soil (Fig. 2a), and the effect of C1 on changes in the SMX concentration in different soil types (Fig. 2b). The results showed that the application of modified biochar significantly improved the removal of SMX (p < 0.01). The three modified biochars (BCA1, YCA1, and RCA1) enhanced SMX removal by 36.5%, 37.7%, and 34.9%, respectively, in black soil. The SMX concentration in the soil was significantly reduced to 0.85–1.40 ng·g^{-1} after 90 d of incubation, and C2 exhibited the best removal efficiency of SMX in black soil. The addition of C1 increased the removal efficiency of SMX in BCA1, YCA1, and RCA1 by 36.5%, 50.2%, and 56.9%, respectively, and was more effective at promoting the removal of pollutants in latosol. In all treatments, SMX concentrations decreased rapidly during the first 30 d and then declined more slowly from Day 30 to Day 90. Black soil amended with modified biochar (BCA) showed the highest SMX removal.

Soil TOC and enzyme activities are shown in Fig. 2c. Under SMX alone, TOC increased slightly in BA (from 3.07 to 3.23 g·kg^{-1}), decreased markedly in YA (from 3.56 to 1.98 g·kg^{-1}), and remained stable in RA. After the addition of biochar, TOC increased in BCA3 (to 4.74 g·kg^{-1}) relative to BA, but decreased in YCA1 (to 1.07 g·kg^{-1}) and RCA1 (to 0.19 g·kg^{-1}) compared with their SMX-only controls. Regarding enzyme activities, SMX alone activated all three enzymes (sucrase, urease, and phosphatase) in black soil, with increases of 26.5%, 77.3%, and 74.0% compared with the control, respectively; however, it generally inhibited enzyme activities in the fluvo-aquic soil and latosol. After the addition of biochar, the sucrase activities in BCA1–BCA3 were all lower than those in BA, but urease and phosphatase remained relatively high, with phosphatase activity in BCA3 (0.235 mg·g^{-1}·24 h^{-1}) being the highest among all treatments. In fluvo-aquic soil, phosphatase in YCA1 (0.192 mg·g^{-1}·24 h^{-1}) was significantly higher than in both YA and CKY (p < 0.001). In latosol, the sucrase, urease, and phosphatase activities in RA were all significantly higher than those in RCA1 (p < 0.01).

Additionally, PARAFAC resolved four fluorescent components from the three-dimensional fluorescence spectra (Supplementary Fig. S2, Supplementary Table S5), with their relative abundances shown in Supplementary Fig. S3. In black and fluvo-aquic soils, SMX alone increased humic-like components (C1–C3) and decreased protein-like C4. After the addition of biochar, this trend remained in black soil, whereas C1 amendment reversed the pattern in fluvo-aquic soil, with C4 recovering to 43.0%. In latosol, SMX alone decreased with C2 and C3 but increased with C4, and the addition of C1 showed no obvious reversal. These results indicate that biochar's effects on DOM composition are soil-type-dependent.

Modified biochar shapes bacterial diversity depending on the soil type and modification method

The effects of biochar on soil bacterial α-diversity are shown in Supplementary Table S6. Overall, modified biochar significantly reduced bacterial richness (ACE and Chao1, p < 0.05) in SMX-contaminated soils, whereas the responses of Shannon's and Simpson's diversity indices varied with the treatment and soil type. In black soil, the ACE and Chao1 indices in BCA1–BCA3 decreased by 23.5%–29.6% and 24.2%–28.9%, respectively, compared with BA, with relatively small differences among the three biochar types. In latosol, biochar exerted a more pronounced effect: the Chao1 index declined by 67.0% (from 1,003.9 ± 429.7 in RA to 331.4 ± 81.0 in RCA1), indicating substantial loss of rare taxa. In fluvo-aquic soil, C1 amendment reduced the Chao1 index by 48.0% relative to YA (from 643.7 ± 184.9 to 334.9 ± 91.7). Notably, the extent of the reduction in richness followed the order latosol > fluvo-aquic soil > black soil, suggesting that the soil's intrinsic properties, rather than biochar

modification type, primarily govern microbial richness responses to modified biochar.

The beta diversity of bacterial communities was analyzed by PCoA at the OTU level combined with PERMANOVA (Fig. 3). The betadisper test (Supplementary Table S7) confirmed that there were no significant differences in multivariate dispersion among the groups (F = 1.3165, p = 0.26), thus satisfying the prerequisites for PERMANOVA analysis. Among all treatment samples (Fig. 3a), PC1 and PC2 explained 24.33% and 16.57% of the community variation (R^2 = 0.9146, p = 0.001). The different soil samples were clearly distinguished, and there were highly significant differences in community structure among the various treatments. Similarly, significant differences were observed among the communities of all treatment groups in black soil (Fig. 3b) (R^2 = 0.9363, p = 0.001), indicating that the addition of SMX and the modification of different biochars can significantly alter the bacterial community's structure in black soil. To further evaluate the impact of soil type, the three soil types were compared under the same C1 treatment (Fig. 3c). The results showed that the three soil types were significantly separated (R^2 = 0.9001, p = 0.003), with the two axes jointly explaining 90.44% of the community variation, confirming that soil type is the primary driver of community differentiation. Overall, soil type, biochar amendment, and addition of SMX all significantly reshaped the bacterial community composition, with soil type having the most pronounced effect.

Biochar-induced shifts in microbial community structure depend on soil type

After 90 d of incubation, all three soil types exhibited distinct dominant phyla (Fig. 4a), including the Firmicutes, Proteobacteria, Actinobacteria, and Chloroflexi. However, the ANCOM-BC2 analysis (Fig. 4b) indicated that the groups showing significant responses were those with lower abundances rather than dominant phyla, and that the effects of different soil types and different modified biochar types differed significantly. In black soil, Acidobacteria was significantly enriched in BCA1 (q < 0.05), whereas Planctomycetes was significantly reduced (q < 0.01). In BCA2, abditibacteriota (FBP) and Gemmatimonadetes were significantly enriched (q < 0.05), whereas in BCA3, unclassified bacteria were significantly reduced (q < 0.05). In fluvo-aquic soil, only unclassified bacteria and Verrucomicrobia were significantly depleted in YCA1 (q < 0.05), whereas the dominant phyla, including Chloroflexi and Actinobacteria, showed no significant changes. In latosol, no phylum reached statistical significance (all q > 0.05).

Responses at the genus level further confirm that the intrinsic properties of the soil determine the extent and direction of biochar-driven microbial reorganization. At the genus level, the dominant genera (relative abundance > 5%) included *Bacillus*, norank_f__Family_XVIII, *Methylobacterium*, *Nocardioides*, *Flavisolibacter*, and *Arthrobacter* (Supplementary Fig. S4). In BA, norank_f__Family_XVIII, *Bacillus*, and *Nocardioides* were the dominant genera (31.62%, 16.05%, and 6.76%, respectively). ANCOM-BC2

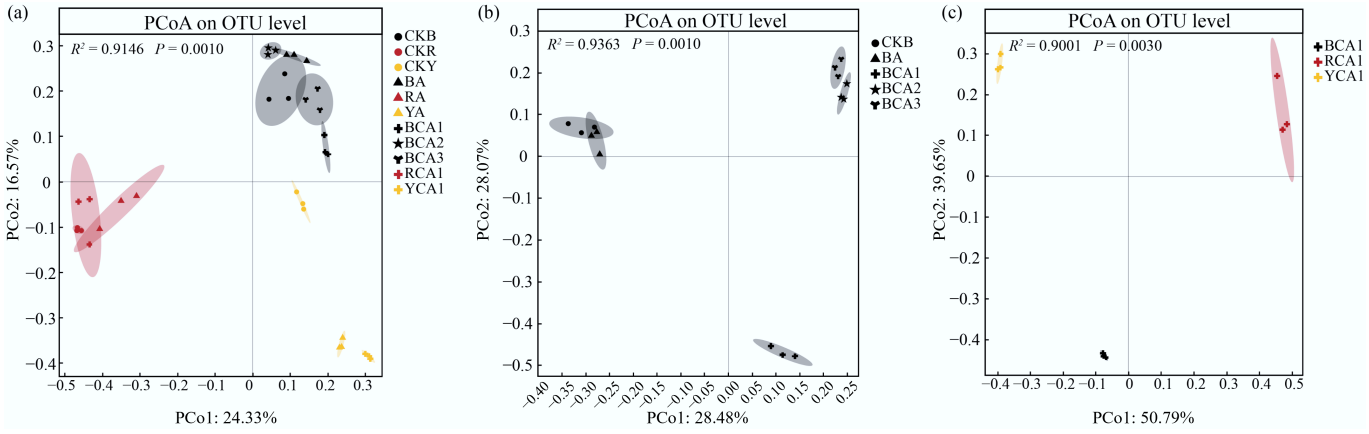


Fig. 3 Beta diversity of microbial communities. (**a**) Comparison of all treatment groups. (**b**) Comparison of all treatment groups in black soil. (**c**) Effects of C1 in different soil types.

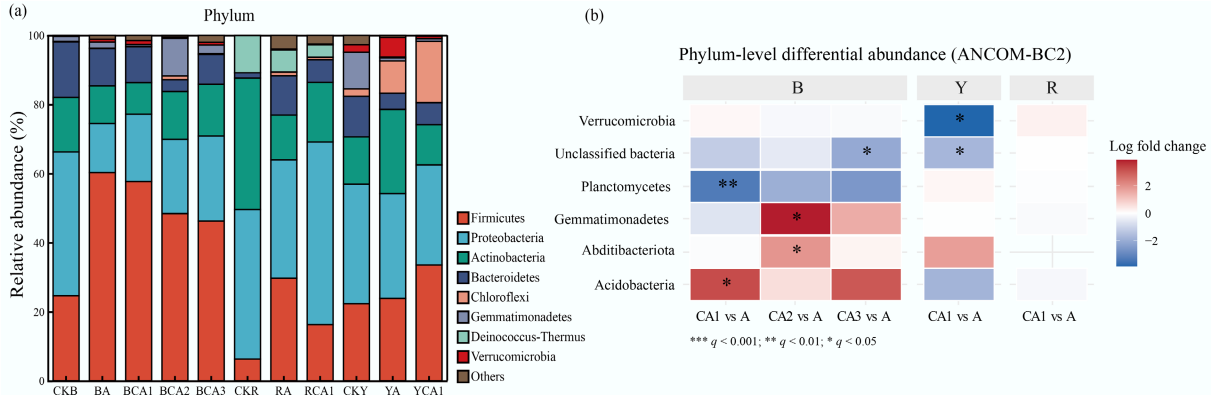


Fig. 4 Phylum-level microbial community composition. (**a**) Relative abundance of dominant phyla. (**b**) Phylum-level differential abundance assessed by ANCOM-BC2. Asterisks denote false discovery rate-adjusted q-values: *** q < 0.001; ** q < 0.01; * q < 0.05.

analysis (Supplementary Fig. S5) showed that *Bacillus* did not reach statistical significance ($q > 0.05$), whereas norank_f__Family_XVIII was significantly depleted in BCA2 and BCA3. The significant genus-level responses in black soil were instead dominated by members of Actinobacteria and Firmicutes. In BCA1, *Micromonospora*, *Streptomyces*, *Microvirga*, *Blastococcus*, and *Flavisolibacter* were significantly enriched, whereas *Skermanella*, *Terrabacter*, *Aestuariimicrobium*, *Brevundimonas*, and *Algoriphagus* were significantly depleted ($q < 0.05$).

In fluvo-aquic soil, ANCOM-BC2 identified 37 genera as significantly differentially abundant between YCA1 and YA. Among these, *Rhodococcus*, *Dietzia*, *Terrabacter*, and *Pontibacter* were significantly enriched, whereas *Arthrobacter*, *Methylobacterium*, *Ellin6055*, and unclassified Family_XVIII were significantly depleted ($q < 0.05$). *Rhodococcus* and *Dietzia* are well-known degraders of organic pollutants, and their enrichment may suggest that biochar enhanced increased the potential for biodegradation in this soil. In latosol, no genus reached statistical significance in the ANCOM-BC2 analysis ($q > 0.05$).

Biochar simplifies microbial networks and alters keystone taxa

The network analysis showed that specific co-occurrence patterns were observed among treatments (Fig. 5a–c). All three networks showed scale-free degree distributions ($R^2 = 0.735–0.765$), small-world properties and modular organization, which are characteristics of complex ecological networks. The degree distributions of the networks followed a power-law model, indicating that most of the nodes had few connections, although a small fraction acted as highly connected hubs[32]. However, their topological features were significantly different (Supplementary Table S8). Network A had the highest average degree (9.838) and total connections (1,579). After the addition of biochar, the network connectivity decreased, with the average degrees (4.803 and 3.105 for CA1 and C1, respectively) and connections (903 and 177 for CA1 and C1, respectively) all decreasing. Conversely, modularity increased from 0.337 in Network A to 0.685 in CA1 and 0.816 in C1, indicating a more compartmentalized network structure where taxa within the same module are more closely associated and may share similar ecological niches.

Although the positive edge ratio was similar between C1 (91.5%) and A (90.2%), it decreased to 58.4% in CA1, with an increase in negative edges (41.6%), indicating that some of the cooperative associations could be substituted by competitive or antagonistic interactions under the combined stress of SMX and biochar. The node-level topological roles were categorized into peripheral nodes, connectors, module hubs, and network hubs on the basis of within-module connectivity (Zi) and among-module connectivity (Pi)[33]. As shown in Fig. 5d, most nodes in all networks were peripherals (88.30%, 63.84%, and 62.93% for A, C1, and CA1, respectively). Network A uniquely contained a network hub, whereas C1 included one module hub. Interestingly, CA1 had more connectors (36) and module hubs (8), suggesting that the addition of biochar under SMX stress enhanced the number of nodes that act as keystone taxa connecting modules or a hub within modules.

The phylogenetic affiliation of these keystone taxa shifted markedly with the addition of biochar. In Network A, the keystone taxa were predominantly Firmicutes, with some Actinobacteria and Bacteroidetes. In network CA1, the keystone taxa shifted toward the dominance of Proteobacteria, including genera such as *Phenylobacterium*, *Mesorhizobium*, unclassified_c__Alphaproteobacteria, and norank_f__Archangiaceae, alongside Firmicutes, Bacteroidetes, and Actinobacteria. Network C1 contained a single module hub from Proteobacteria. Module hubs and connectors are thought to act as keystone species that strongly influence an ecosystem's functioning and stability[33,34]. The transition from Firmicutes- to Proteobacteria-dominated keystone taxa may suggest that modified biochar, particularly under SMX stress, selects for different ecological strategies, favoring taxa often associated with xenobiotic degradation and nutrient cycling.

Biochar amendment partially recovers predicted SMX-suppressed metabolic functional potential

To further elucidate the functional responses of soil bacterial communities to SMX and biochar, PICRUSt was used to predict Level 2 Kyoto Encyclopedia of Genes and Genomes (KEGG) metabolic functions for the A, C1, and CA1 treatments (Fig. 6). Carbohydrate metabolism, amino acid metabolism, and energy metabolism were the dominant functional categories across all treatments and exhibited high relative abundances with relatively modest variation.

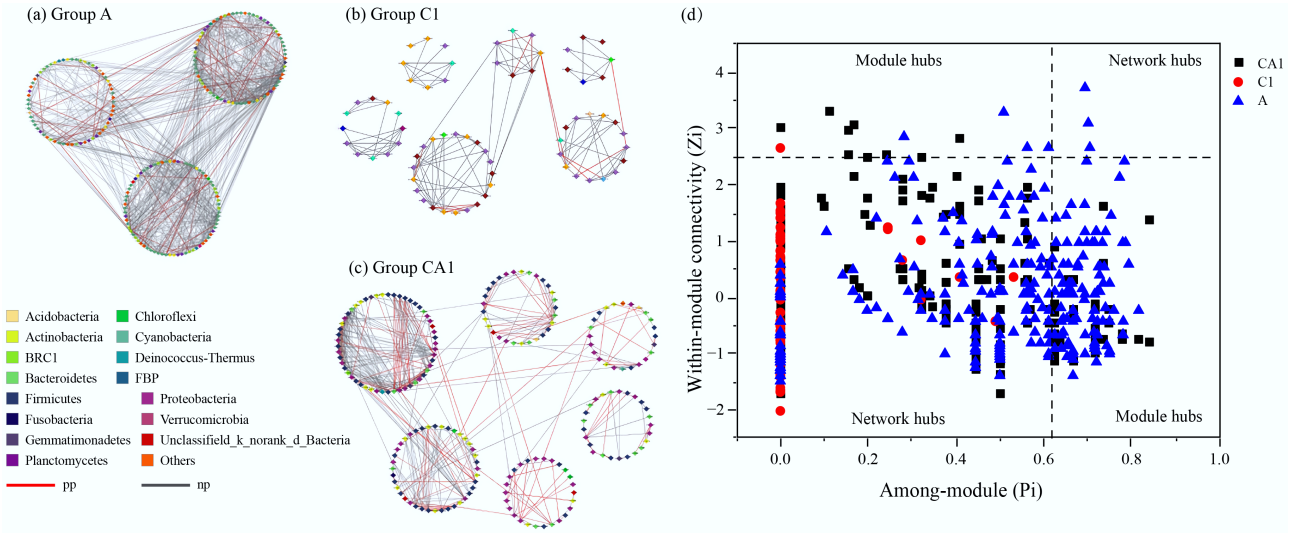


Fig. 5 Diagram of the soil bacterial molecular ecological network under three treatments. (**a**–**c**) Each node represents a bacterial OTU; red lines indicate positive interactions between nodes (pp), and gray lines indicate negative interactions between nodes (np). (**d**) Distribution of within-module connectivity–among-module connectivity (Zi–Pi) values for nodes in the microbial network.

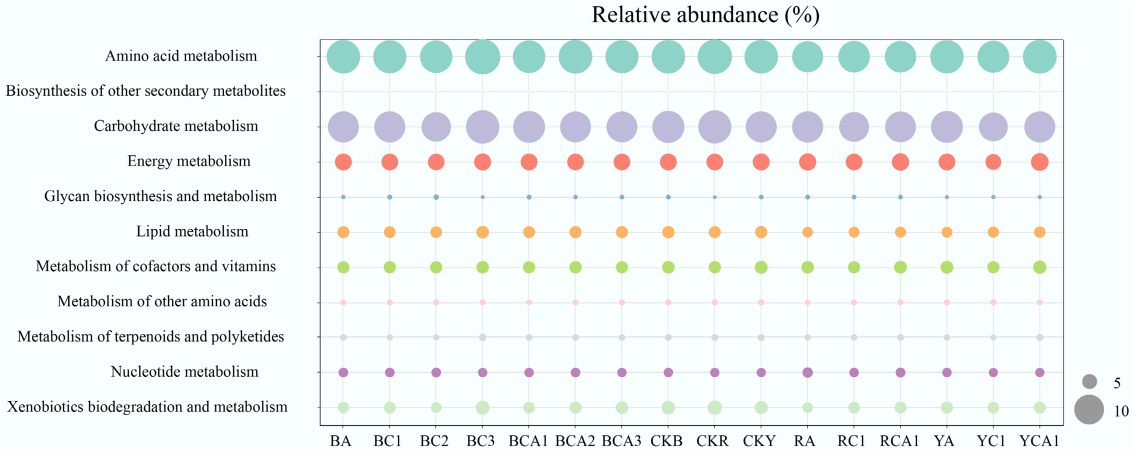


Fig. 6 PICRUSt function prediction.

Compared with the controls, addition of SMX suppressed the predicted functional potential of carbohydrate and amino acid metabolism, as well as xenobiotic biodegradation pathways. Modified biochar alleviated these inhibitions, partially or fully restoring metabolic functions to control levels while enriching xenobiotic biodegradation functions. However, the extent of recovery varied, depending on the soil type. The predicted abundance of functional genes in black soil under the CA1 treatment remained slightly lower than that in the control group, whereas it fully recovered in latosol. This predicted functional restoration coincided with an enrichment of Actinobacteria, a phylum associated with xenobiotic degradation and nutrient cycling[35], suggesting that biochar-induced shifts in community structure are closely linked to the recovery of key metabolic pathways. Notably, the PICRUSt-based predictions reflect genomic potential rather than actual metabolic activity; metatranscriptomic or metabolomic analyses would be required for confirmation.

Discussion

Soil type governs microbial and remediation responses to biochar

Modified biochar reduced microbial richness in SMX-contaminated soils, likely because the efficient sequestration of SMX decreased the selective pressure for a broad range of SMX-tolerant taxa[36]. In contrast, soils receiving SMX alone exhibited higher microbial richness, suggesting that the relatively low SMX concentration (20 ng·g^{-1}) may have acted as a mild stressor that stimulated microbial activity and proliferation rather than causing toxicity[37]. This stimulating effect at low concentrations of antibiotics has been previously reported in agricultural soils[38], confirming the hormesis-like response observed here.

In black soil, the three modified biochars (C1, C2, C3) reduced microbial diversity without significant differences, indicating that the type of biochar modification did not strongly affect microbial richness under the conditions tested but the soil type had a greater effect. The greatest reduction was observed in latosol, followed by fluvo-aquic soil, but the smallest reduction was found in black soil. This soil type-dependent pattern is consistent with meta-analysis studies reporting that soil properties such as pH and organic matter content modulate the effect of biochar on microbial communities[17,18]. For instance, the three soils involved in this study had significant differences in their basic properties, in which latosol had the lowest pH and organic carbon content (Supplementary Table S2). The greatest decrease in bacterial richness was found in this acidic and nutrient-poor soil, indicating that low pH and carbon availability may enhance the selective pressure of biochar on the microbial community, which is consistent with previous studies reporting the stronger effect of biochar amendment in acidic soils[13,34].

Biochar can change the soil's physicochemical properties significantly, thus restructuring the bacterial community's structure[39–41]. Zhu et al.[42] further corroborated these findings, reporting that shifts in the bacterial community's composition following modified biochar were positively correlated with soil pH, organic carbon, and nitrogen content. The soil type-dependent shifts were also reflected in the composition of DOM and enzyme activities. In black soil, SMX alone increased humic-like components and activated sucrase, urease, and phosphatase, whereas in latosol, it decreased humic-like components and inhibited enzyme activities, further supporting the idea that soil properties modulate biochar's effects on microbial function.

It should be noted that chemical modification of biochar may introduce substances with potential ecological risks. CTAB is a cationic surfactant that may be toxic to nontarget soil organisms at high concentrations, whereas $FeCl_3$ modification may release Fe ions and acidify the soil microenvironment[25]. However, since the application rate of biochar in this study was 1% (by mass), adverse effects are limited. Before field-scale application, long-term ecological safety assessments, including evaluations of the impacts on soil fauna and flora, should be conducted.

Biochar simplifies microbial networks and enriches functional degrading taxa

The addition of biochar reduced microbial richness while simplifying and modularizing the co-occurrence networks. Under SMX stress alone, the microbial networks were more complex, with higher connectivity and interaction density. The increased complexity can be attributed to the large number of diverse cooperative interactions among taxa participating in SMX's transformation and stress mitigation[3]. Conversely, the addition of biochar decreased network connectivity and increased modularity, indicating a more compartmentalized structure with fewer but tightly interconnected modules. This simplification is consistent with the observed decrease in richness and may suggest that biochar alleviated the overall antibiotic stress by efficiently adsorbing SMX, thus reducing the need for broad synergistic responses among taxa.

Concurrently, biochar acted as a selective environmental filter, enriching functional bacterial groups related to antibiotic degradation and enhancing predicted metabolic potential. In particular, Acidobacteria was significantly enriched in biochar-amended black soil, and the keystone taxa within the co-occurrence networks shifted from Firmicutes to Proteobacteria. These groups have been frequently associated with xenobiotic degradation and the cycling of carbon and nitrogen, and their enrichment may suggest a potential capacity for SMX attenuation and nutrient transformation. Among these, *Streptomyces* and *Rhodococcus* have been reported to be sulfonamide-degrading bacteria[43,44].

Compared with Gram-positive bacteria, Gram-negative bacteria have an outer membrane which acts as an extra barrier to external stressors, thus providing higher tolerance or resistance to many toxic compounds[45,46]. This structural advantage may explain why Proteobacteria-affiliated taxa became keystone species in the biochar-amended networks, even though their overall abundance did not change significantly, because this phylum is largely composed of Gram-negative species. Direct measurements of membrane permeability or efflux activity under SMX stress would provide stronger support for this interpretation. The enrichment of Proteobacteria which contains many denitrifying taxa and carbon-degrading bacteria may therefore improve the soil ecosystem's functions by potentially accelerating nitrogen and carbon cycling in SMX-contaminated soils[47].

The responses to biochar were also soil type-dependent. Microbial community composition and network structure in black and fluvo-aquic soils showed more pronounced changes after the addition of biochar than those in latosol, including a stronger enrichment of putative SMX-degrading taxa, especially in black soil. These findings highlight that biochar-driven simplification of microbial networks is accompanied by a functional reassembly of key degrading taxa, and that the magnitude of these effects is governed by the soil type. However, network analysis reveals co-occurrence patterns rather than direct causal interactions. Functional inferences based on taxonomy remain speculative and require validation. Nevertheless, the clear beta diversity separations among soils and biochars (Fig. 3) suggest that the network structures are also soil- and modification-dependent.

Higher SMX removal can be attributed to adsorption and stimulated microbial metabolism

The significantly enhanced removal of SMX in biochar-amended soils can be attributed to the combined contribution of abiotic adsorption and biotic processes. On the abiotic side, modified biochars possessed a higher density of well-developed pores, providing more adsorption sites and thereby increasing the sorption capacity for SMX. In this context, π–π electron donor–acceptor interactions are a key mechanism underlying the adsorption of aromatic antibiotics by biochar. SMX contains N/O aromatic heterocycles and sulfonamide groups with strong electron-withdrawing ability, whereas the conjugated π systems in biochar are electron donors, which is conducive to π–π interaction and promotes the sorption of SMX[48,49]. Additionally, oxygen-containing functional groups introduced or reorganized in the modification process (e.g., phosphate and Fe–O-related groups) can form hydrogen bonding or surface complexes with SMX, further improving the adsorption efficiency[50].

Following the rapid initial adsorption, the biotic processes take effect. Functional prediction analyses predicted that pathways associated with xenobiotic biodegradation, energy metabolism, and carbon and nitrogen cycling were relatively more abundant in biochar-amended soils compared with the conditions without SMX. Biochar immobilizes SMX by adsorption and creates a more favorable environment for microbial activity, which may improve metabolic processes and facilitate the biodegradation of residual SMX. Remediation in biochar-amended soils may be jointly driven by the enrichment and activation of functional microbial populations and by strong initial adsorption to the biochar's surfaces. This phenomenon, characterized by a rapid initial decline in the SMX concentration followed by a slower sustained decrease, is consistent with a dual mechanism involving both abiotic and biotic processes. The enhanced metabolic activity was supported by increased TOC, elevated enzyme activities, and shifts in the DOM composition in biochar-amended soils, particularly in black soil, consistent with the higher SMX removal observed.

However, our experimental design does not allow quantitative separation of the two processes. Future studies using isotopically labeled SMX or sterilized controls are needed to determine their relative contributions. The surface properties of the biochar in this study were characterized mainly by SEM, EDS, and FTIR. The interpretations regarding pore development, iron oxide formation, and surface charge remain preliminary speculations. Future studies should incorporate Brunauer–Emmett–Teller analysis, XRD, and zeta potential measurements to quantitatively validate these properties.

Implications for precision remediation: a soil-specific biochar matching framework

This study provides experimental support for developing a precision remediation framework based on soil-specific biochar matching. Our results show that C1 performed differently across the three soil types. Because C2 and C3 were tested only in black soil, we cannot determine whether they would outperform C1 in fluvo-aquic soil or latosol. In latosol, C1 addition enhanced the removal of SMX to a greater extent than in the other two soils, whereas in black soil, biochar-induced shifts in the community structure and the enrichment of potential SMX degraders were more pronounced. These patterns highlight the lack of a universal "best" biochar and emphasize the necessity of matching biochar's properties with specific soil conditions to optimize remediation efficiency and cost-effectiveness.

Practically, this implies that the selection and design of biochar for microbial remediation should be based on key soil properties rather than applying a uniform amendment across different soil types. Future work should be directed toward the assessment of soil pH, organic matter, mineralogy, and nutrient status to identify or design biochars with an appropriate surface chemistry and porosity for each target soil. Such a customized approach can guarantee that biochar will effectively adsorb pollutants such as SMX and also modulate the local microbiome optimally by restructuring the microbial interaction networks and restoring key metabolic functions, thus facilitating synergistic and sustainable soil restoration.

Conclusions

In summary, the addition of biochar revived the soil's vitality and successfully remediated antibiotic-contaminated soil. Nevertheless, in black soil, different modified biochars exerted differential effects on the recovery of the microecology, and C1 showed soil-type-dependent performance across the three soils. Biochar types enriched different antibiotic-degrading functional bacteria, thereby facilitating the efficient removal of SMX. Soil type strongly influenced the performance of C1, whereas the comparison among modification methods was restricted to black soil. Among the various soils, the decline in microbial richness was most pronounced in latosol after the addition of biochar, but the response of microbes to biochar was most intense in black soil. Biochar primarily restored the soil and repaired

antibiotic pollution by enriching functional bacterial strains and optimizing microbial network structures, reducing internal microbial competition while enhancing energy and metabolic processes within the network. Therefore, when using biochar for the remediation of contaminated soils in the future, it is essential to consider the type of soil for precise matching of the biochar modification methods.

Supplementary information

It accompanies this paper at: https://doi.org/10.48130/bchax-0026-0023.

Ethical statements

Not applicable. This study does not involve human or animal subjects. During the preparation of this work, the authors used DeepSeek solely for language polishing and improving the grammar. DeepSeek was not used for data analysis, data interpretation, figure preparation, or generating scientific content. After using this tool, the authors reviewed and edited the content as needed and take full responsibility for the integrity and originality of the final manuscript.

Author contributions

The authors confirm their contributions to the paper as follows: Caicai Xie: formal analysis, investigation, data curation, software, writing – original draft, writing – review and editing; Yuye Zhang: formal analysis, investigation, data curation, software, validation, writing – review and editing; Tianci Tang: data curation, methodology, software, writing – review and editing; Siqi Tong: investigation, data curation, software, writing – review and editing; Ruonan Wang: data curation, investigation, methodology, software, writing – review and editing; Shichao Ma: formal analysis, methodology, software, writing – review and editing; Xiaohui Liu: funding acquisition, project administration, methodology, supervision, writing – original draft, writing – review and editing; Fengmin Li: formal analysis, conceptualization, visualization, supervision, writing – review and editing; Changbing Ye: conceptualization, methodology, supervision, validation, writing – review and editing; Bin Zhao: conceptualization, methodology, supervision, validation, writing – review and editing; Ying Liu: data curation, conceptualization, funding acquisition, project administration, supervision, resources, writing – review and editing. All authors reviewed the results and approved the final version of the manuscript.

Data availability

The datasets generated and/or analyzed during the current study are available from the corresponding author on reasonable request.

Acknowledgments

Not applicable.

Funding

This work was financially supported by the National Natural Science Foundation of China (Nos. 42677287 and 42207260), Shandong Provincial Natural Science Foundation (ZR2026MS0510, ZR2024QD023, and ZR2025QC1122), and Taishan Scholars Program of Shandong Province (Nos. tsqn202312094 and tsqnz20250721).

Declarations

Competing interests

The authors declare that they have no known competing financial interests or personal relationships that could have appeared to influence the work reported in this paper.

Author details

[1]Key Laboratory of Marine Environment and Ecology, Ministry of Education and College of Environmental Science and Engineering, Ocean University of China, Qingdao 266100, China; [2]College of Chemical and Environmental Engineering, Yuxi Normal University, Yuxi 653100, China; [3]School of Environment and Geography, Shandong Key Laboratory of Synergistic Control of Complex Mult-Media Pollution, Shandong Key Laboratory of Polymeric Materials Recycling and Upcycling, Qingdao University, Qingdao 266071, China

References

[1] Zhang R, Zheng X, Chen B, Ma J, Niu X, et al. 2020. Enhanced adsorption of sulfamethoxazole from aqueous solution by Fe-impregnated graphited biochar. *Journal of Cleaner Production* 256:120662

[2] Li J, Zhao L, Feng M, Huang CH, Sun P. 2021. Abiotic transformation and ecotoxicity change of sulfonamide antibiotics in environmental and water treatment processes: a critical review. *Water Research* 202:117463

[3] Archundia D, Martins JMF, Lehembre F, Morel MC, Duwig C. 2021. Sulfamethoxazole biodegradation and impacts on soil microbial communities in a Bolivian arid high altitude catchment. *Chemosphere* 284:131335

[4] Kong S, Zhao YG, Guo L, Gao M, Jin C, et al. 2020. Transcriptomics of *Planococcus kocurii* O516 reveals the degrading metabolism of sulfamethoxazole in marine aquaculture wastewater. *Environmental Pollution* 265:114939

[5] Wang J, Zhuan R. 2020. Degradation of antibiotics by advanced oxidation processes: an overview. *Science of the Total Environment* 701:135023

[6] Dikšaitytė A, Kacienė G, Miškelytė D, Januškaitienė I, Sujetovienė G, et al. 2025. Exacerbated toxicity of sulfamethoxazole in growth and photosynthetic performance of *Hordeum vulgare* under future climate scenario. *Environmental Research* 282:122041

[7] Ouyang P, Narayanan M, Shi X, Chen X, Li Z, et al. 2023. Integrating biochar and bacteria for sustainable remediation of metal-contaminated soils. *Biochar* 5:63

[8] Srinivasan P, Sarmah AK. 2015. Characterisation of agricultural waste-derived biochars and their sorption potential for sulfamethoxazole in pasture soil: a spectroscopic investigation. *Science of the Total Environment* 502:471–480

[9] Rajapaksha AU, Vithanage M, Lim JE, Ahmed MBM, Zhang M, et al. 2014. Invasive plant-derived biochar inhibits sulfamethazine uptake by lettuce in soil. *Chemosphere* 111:500–504

[10] Hu F, Gao C, Wang B, Ding Z, Zhang L, et al. 2024. Effects of chicken manure-modified biochar on the adsorption capacity of tetracycline and abundance of antibiotic resistance genes in soil. *Land Degradation & Development* 35:1224–1233

[11] Du Z, Sun X, Zheng S, Wang S, Wu L, et al. 2024. Optimal biochar selection for cadmium pollution remediation in Chinese agricultural soils via optimized machine learning. *Journal of Hazardous Materials* 476:135065

[12] Liu X, He Y, Li J, Li J, Zhang J, et al. 2025. Does biochar field aging reduce the kinetic retention for weakly hydrophobic antibiotics in purple soil? *Biochar* 7:69

[13] Zhang M, Riaz M, Zhang L, El-desouki Z, Jiang C. 2019. Biochar induces changes to basic soil properties and bacterial communities of different soils to varying degrees at 25 mm rainfall: more effective on acidic soils. *Frontiers in Microbiology* 10:1321

[14] Singh H, Northup BK, Rice CW, Prasad PVV. 2022. Biochar applications influence soil physical and chemical properties, microbial diversity, and crop productivity: a meta-analysis. *Biochar* 4:8
[15] Wang H, Zhang R, Zhao Y, Shi H, Liu G. 2022. Effect of biochar on rhizosphere soil microbial diversity and metabolism in tobacco-growing soil. *Ecologies* 3:539–556
[16] Xu W, Whitman WB, Gundale MJ, Chien CC, Chiu CY. 2021. Functional response of the soil microbial community to biochar applications. *GCB Bioenergy* 13:269–281
[17] Li X, Wang T, Chang SX, Jiang X, Song Y. 2020. Biochar increases soil microbial biomass but has variable effects on microbial diversity: a meta-analysis. *Science of the Total Environment* 749:141593
[18] Wang M, Yu X, Weng X, Zeng X, Li M, et al. 2023. Meta-analysis of the effects of biochar application on the diversity of soil bacteria and fungi. *Microorganisms* 11:641
[19] Xu W, Xu H, Delgado-Baquerizo M, Gundale MJ, Zou X, et al. 2023. Global meta-analysis reveals positive effects of biochar on soil microbial diversity. *Geoderma* 436:116528
[20] Minaei S, Zoroufchi Benis K, McPhedran KN, Soltan J. 2024. Adsorption of sulfamethoxazole and lincomycin from single and binary aqueous systems using acid-modified biochar from activated sludge biomass. *Journal of Environmental Management* 358:120742
[21] Xu X, Weng Y, Zhuang J, Pei H, Wu B, et al. 2024. Enhanced adsorption capacity of antibiotics by calamus-biochar with phosphoric acid modification: performance assessment and mechanism analysis. *Journal of the Taiwan Institute of Chemical Engineers* 161:105541
[22] Egbedina AO, Ugwuja CG, Dare PA, Sulaiman HD, Olu-Owolabi BI, et al. 2023. CTAB-activated carbon from peanut husks for the removal of antibiotics and antibiotic-resistant bacteria from water. *Environmental Processes* 10:20
[23] Hua Z, Pan Y, Hong Q. 2023. Adsorption of Congo red dye in water by orange peel biochar modified with CTAB. *RSC Advances* 13:12502–12508
[24] Zeng S, Choi YK, Kan E. 2021. Iron-activated bermudagrass-derived biochar for adsorption of aqueous sulfamethoxazole: effects of iron impregnation ratio on biochar properties, adsorption, and regeneration. *Science of the Total Environment* 750:141691
[25] Cheng H, Xing D, Lin S, Deng Z, Wang X, et al. 2022. Iron-modified biochar strengthens simazine adsorption and decreases simazine decomposition in the soil. *Frontiers in Microbiology* 13:901658
[26] Hernández-Sánchez N, Lleó L, Ammari F, Cuadrado TR, Roger JM. 2017. Fast fluorescence spectroscopy methodology to monitor the evolution of extra virgin olive oils under illumination. *Food and Bioprocess Technology* 10:949–961
[27] Stedmon CA, Bro R. 2008. Characterizing dissolved organic matter fluorescence with parallel factor analysis: a tutorial. *Limnology and Oceanography: Methods* 6:572–579
[28] Weaver RW, Angle S, Bottomley P, Bezdicek D, Smith S, et al. 1994. *Methods of Soil Analysis, Part 2: Microbiological and Biochemical Properties*. USA: Soil Science Society of America. doi: 10.2136/sssabookser5.2
[29] Liu X, Lu S, Liu Y, Wang Y, Guo X, et al. 2021. Performance and mechanism of sulfamethoxazole removal in different bioelectrochemical technology-integrated constructed wetlands. *Water Research* 207:117814
[30] Tan L, Xiao Y, Zeng WA, Gu S, Zhai Z, et al. 2022. Network analysis reveals the root endophytic fungi associated with Fusarium root rot invasion. *Applied Soil Ecology* 178:104567
[31] Wang X, Sato T, Xing B. 2006. Competitive sorption of pyrene on wood chars. *Environmental Science & Technology* 40:3267–3272
[32] Kong X, Cernava T, Wang Y, Jin D. 2023. Native fungal community remains resilient during bioremediation of DBP pollution by exogenous *Gordonia phthalatica* QH-11^T. *Science of the Total Environment* 892:164532
[33] Shi S, Nuccio EE, Shi ZJ, He Z, Zhou J, et al. 2016. The interconnected rhizosphere: high network complexity dominates rhizosphere assemblages. *Ecology Letters* 19:926–936
[34] Yuan MM, Guo X, Wu L, Zhang Y, Xiao N, et al. 2021. Climate warming enhances microbial network complexity and stability. *Nature Climate Change* 11:343–348
[35] BhinsaraVM. 2026. Actinobacteria mediated bioremediation of pesticide and heavy metal contaminated soils using omics and emerging strategies. *Discover Environment* 4:413
[36] Liang J, Tang S, Gong J, Zeng G, Tang W, et al. 2020. Responses of enzymatic activity and microbial communities to biochar/compost amendment in sulfamethoxazole polluted wetland soil. *Journal of Hazardous Materials* 385:121533
[37] Fér M, Kodešová R, Kalkušová B, Klement A, Nikodem A. 2020. An empirical model for describing the influence of water content and concentration of sulfamethoxazole (antibiotic) in soil on the total net CO_2 efflux. *Journal of Hydrology and Hydromechanics* 68:351–358
[38] Liu Y, Li R, Xiao X, Wang Z. 2019. Bacterial metabolism-inspired molecules to modulate antibiotic efficacy. *Journal of Antimicrobial Chemotherapy* 74:3409–3417
[39] Fan S, Zuo J, Dong H. 2020. Changes in soil properties and bacterial community composition with biochar amendment after six years. *Agronomy* 10:746
[40] Lang Q, Guo X, Zou G, Wang C, Li Y, et al. 2023. Hydrochar reduces oxytetracycline in soil and Chinese cabbage by altering soil properties, shifting microbial community structure and promoting microbial metabolism. *Chemosphere* 338:139578
[41] Zhang L, Jing Y, Xiang Y, Zhang R, Lu H. 2018. Responses of soil microbial community structure changes and activities to biochar addition: a meta-analysis. *Science of the Total Environment* 643:926–935
[42] Zhu Z, Zhang Y, Tao W, Zhang X, Xu Z, et al. 2025. The biological effects of biochar on soil's physical and chemical characteristics: a review. *Sustainability* 17:2214
[43] Sarnthima R, Mongkolthanaruk W, Sanachai K, Khammuang S. 2024. Laccase from *Streptomyces* sp. CS29 and molecular insight of sulfamethoxazole degradation. *Biologia* 79:311–320
[44] Larcher S, Yargeau V. 2011. Biodegradation of sulfamethoxazole by individual and mixed bacteria. *Applied Microbiology and Biotechnology* 91:211–218
[45] Breijyeh Z, Jubeh B, Karaman R. 2020. Resistance of gram-negative bacteria to current antibacterial agents and approaches to resolve it. *Molecules* 25:1340
[46] Richter MF, Drown BS, Riley AP, Garcia A, Shirai T, et al. 2017. Predictive compound accumulation rules yield a broad-spectrum antibiotic. *Nature* 545:299–304
[47] Jing H, Li J, Yan B, Wei F, Wang G, et al. 2021. The effects of nitrogen addition on soil organic carbon decomposition and microbial C-degradation functional genes abundance in a *Pinus tabulaeformis* forest. *Forest Ecology and Management* 489:119098
[48] Kang Z, Jia X, Zhang Y, Kang X, Ge M, et al. 2022. A review on application of biochar in the removal of pharmaceutical pollutants through adsorption and persulfate-based AOPs. *Sustainability* 14:10128
[49] Peiris C, Gunatilake SR, Mlsna TE, Mohan D, Vithanage M. 2017. Biochar based removal of antibiotic sulfonamides and tetracyclines in aquatic environments: a critical review. *Bioresource Technology* 246:150–159
[50] Anuar NF, Iskandar Shah DRS, Ramli FF, Md Zaini MS, Mohammadi NA, et al. 2023. The removal of antibiotics in water by chemically modified carbonaceous adsorbents from biomass: a systematic review. *Journal of Cleaner Production* 401:136725

Copyright: © 2026 by the author(s). Published by Maximum Academic Press, Fayetteville, GA. This article is an open access article distributed under Creative Commons Attribution License (CC BY 4.0), visit https://creativecommons.org/licenses/by/4.0/.